Flap deflection* tests were performed for the basic models (8-13) at a speed of 40 feet per second. Flap deflection conditions were defined as zero, one-third, two-third, and full. No precise measurements were made as to the exact angle of flap deflection. However, a zero flap condition corresponds to maintaining the Parafoil chord line straight, a full flap condition is indicative of a flap deflection of about 75^{O} with the horizontal, one-third, about 25^{O}, and two thirds about 50^{O}.

The tests yielded lift and drag data versus angle of attack.

Strut Testing Phase. The Strut Testing set-up is given in Figures 28 and 30. The suspension lines were cut a distance approximately 33.9% from the flares to permit the Parafoil to fly essentially at the tunnel center-line. These lines were then attached to a metal grid framework. The grid was attached to a strut mounting system extending from the groundboard. Two strain gauge balances were positioned on the bottom surface of the Parafoil at the quarter-chord locations on each side, in addition to various gauges located beneath the groundboard which yielded all the force and moment coefficients. The groundboard was mounted on a turntable, which could be rotated for data acquisition as the model was yawed.

Unlike the tether testing phase, the model control lines were attached to the grid, and could be adjusted according to flap deflections desired. Tufts of wool were attached to the top cambered surface to assist visual analysis of the flow field (Figure 31).

The grid and mounting arrangement for each model was first "tested" with the Parafoil removed. By recording the force and moment effects due to the mounting apparatus, this effect was then removed from the wing-line data. As a data point was recorded the angle of attack was measured by two methods: (1) by photographing the main strut support (this support was attached perpendicular to the Parafoil chord line at the models mid-span); and (2) by visually observing the near-side Parafoil chord line. The angle of attack was varied mechanically by rotating the strut grid. Hence an angle of attack range from -10^{O} to 80^{O} was achieved.

Parafoil models 8, 10, and 12 (AR 1.0, 2.0, 3.0) were tested extensively at a tunnel speed of 40 feet per second yielding the longitudinal coefficients C_L, C_D, and C_m, and the lateral-directional coefficients: C_Y, C_n, and C_l. Longitudinal data only was recorded for model 9 (AR 1.5) at tunnel speeds of 30, 40, 50 and 60 feet per second. Model 11 (AR 2.5) was tested at 40 feet per second yielding longitudinal data. Models 8, 10, and 12 were tested at various flap deflection conditions defined as zero, one-half, and full. A zero flap condition corresponds to maintaining a straight Parafoil chord line, a full flap condition corresponds to a flap deflected about 75^{O} with the horizontal and a half flap condition, about 37.5^{O}.

*The rear 25% of the wing area is deflected by pulling in the control lines across the entire span.

Data Reduction

Notre Dame

Static Tests. The Notre Dame static model configurations yielded the lift and drag forces measured by the balance system. The signals from the strain gauge were channeled to potentiometers where the lift and drag forces were read independently of each other. This technique involved a calibration and balancing of circuits, and a conversion of milli-volt readings to pounds. The drag measured by the balance included the drag of the metal sting on which the model was mounted. This drag contribution was then subtracted from the total drag, yielding the aerodynamic force of the wing itself. The angle of attack was measured by means of a protractor dial and correlated with the lift and drag measurements.[6,7]

Dynamic Tests. The reduction of data obtained through dynamic tests was accomplished in the following manner. A polaroid picture representing one trim position of the Parafoil model was analyzed to determine (1) the angle of trim, α_T*, and (2) the angle, γ, as shown in Figure 26. This information was tabulated for that specific test run to later compare with the results of the dynamic analysis.

The 16mm high speed film documenting the oscillatory motion of the Parafoil was processed to a negative print from which the Parafoil motion in degrees was read directly. By using a stop-frame projector, the pointer position in each frame of the film was read in angular degrees to within an accuracy of .25 degrees. The change in the pitch angle, θ, with time was determined by utilizing the camera film speed (128 frames/sec).

The zero position of the angle indicator was aligned with the x-axis in the wind tunnel thereby permitting the direct determination of the angle of attack from the position of the pointer.

Now that the motion has been reduced to a set of angles at known increments of time this data was then fitted to the following equation:[9]

$$\alpha = Ke^{\lambda t} \cos(\omega t + \delta) + \alpha_T$$

Writing the above equation in symbolic form,

$$\alpha = f(\alpha_T, t, K, \lambda, \omega, \delta)$$

---

* $\alpha_T = K_3$, $\theta = \alpha$.

This equation consists of two variables (angle of attack and time) and four undetermined constants which are

K - maximum amplitude
λ - damping rate
ω - angular frequency
δ - phase angle

By using the Method of Differential Corrections and obtaining the initial approximation for the four constants from the plotted data, the constants are determined.

The first approximations for the various constants were determined in the following manner from the plotted data (θ vs time).

(1) α_T was determined as the mean of the two extreme points of minimum amplitude.

(2) $\omega = \frac{(n-1)\pi}{t_n}$

where n is the number of extreme points and t_n is the time interval between the first and last of the extreme points.

(3) δ is determined as $\delta = \omega t_o$ where t_o is the time interval between the normalized time zero (middle point of sections of data being fitted) and the preceding positive maximum.

(4) K is determined as the distance from the α_T line to the intercept at normalized time zero of the envelope of positive maximum points.

(5) $\lambda = 0$

An example of the oscillatory motion of a typical test run is presented in Figure 32 with the first approximations shown.

The "WOBBLE PROGRAM",[9] was used to extract representative values for K, λ, ω and α_T as functions of time from the pitching motion of the Parafoil. Using these computed values along with the lateral moment of inertia, I, of the Parafoil and suspension system, the wind velocity, and the Parafoil characteristic length and area, the stability coefficients C_{m_α} and $C_{m_q} + C_{m_{\dot\alpha}}$ were determined as functions of time from the following equations.

$$C_{m_\alpha} = -2\omega^2 I / \rho V^2 Sc$$

$$C_{m_q} + C_{m_{\dot{\alpha}}} = {}^{8\lambda I}/_{\rho VSc^2}$$

By employing overlapping sectional fits in the data reduction technique, a means of investigating the non-linearities of the stability coefficients with angle of attack is provided.

NASA Langley (Series One)

The data obtained through this test program was taken from reference 3, and represents the forces and moments characteristics of the Parafoil systems. For comparison purposes the force data was referred to the basic Parafoil by removing the suspension line drag as explained in Appendix II.

NASA Langley (Series Two)

Langley presented the data obtained to the University of Notre Dame for analysis in tabular coefficient form representing the system as tested, uncorrected for unexposed suspension lines. Because the mounting technique resulted in a percentage of the suspension lines being unexposed to the airstream, (tether phase) or a percentage being cut off (strut phase), the entire drag force was not measured. Hence this data was corrected according to two different approaches dictated by the analysis desired.

The first approach considered the removal of the drag due to the suspension line lengths exposed to the airstream. Hence the corrected data resulted in the drag of the Parafoil alone and serves as an excellent method of comparing the aerodynamic characteristics of the Parafoils to one another. The procedure was to determine the length and number of suspension lines exposed to the airstream. Knowing the diameter of the lines (under tension), the projected frontal area was computed. Assuming a drag coefficient of 1.0 based on the line frontal area,[10] the drag coefficient based on wing area was determined. This line drag coefficient was then subtracted from the given test drag coefficient, and resulted in the drag coefficient of the Parafoil itself. For a more detailed treatment refer to Appendix II.

The second approach considered the addition of the drag due to the suspension line lengths not exposed to the air flow. The procedure is very much similar to the former case but results in the drag of the total system-Parafoil and suspension lines. For a more concise treatment of this approach refer to Appendix III.

Wind tunnel data from all of the test programs was punched onto IBM computer cards and programmed for various operations on the University of Notre Dame Univac digital computer, Model 1107. Thus, the results could then be plotted by the computer in any desired manner.

ANALYSIS OF RESULTS

Early Notre Dame Tests

The first wind tunnel tests were carried out on a completely fabric model of an original Parafoil kite modified for wind tunnel testing. The unit was placed in the wind tunnel with flow visualization made possible by the use of smoke streamlines. The flow field over the Parafoil was observed. Special attention was given to the location of the stagnation points, separation of the flow, three dimensional effects due to the flares, general rigidity, and stability characteristics. Figures 2 and 33 show some of these smoke flow pictures.

Following these flow visualization tests the first Parafoil wind tunnel model was constructed and tested. This wind tunnel model is described in the section on the model description (Model 1). Summary curves of the aerodynamic data for the flexible unit is given in Figures 34 and 35 as the AR 0.83 traces.

Extensive wind tunnel tests were also carried out on all rigid models of the Parafoil.[6] Results for the all rigid model wind tunnel tests were compared with data obtained on a rigid airfoil model (no openings in the leading edge). Wind tunnel tests were also carried out where fabric cloth was placed over the rigid model and also used as flares. Summary curves for this rigid Parafoil model (Model 2) are given in Figures 34 and 35 as the AR 1.77 traces.

A summary of the effects of the rigid airfoil and its model variations is presented inFigure 36*. A summary of the effects of the rigid Parafoil and its model variation is presented in Figure 37.*-** In addition, Figure 37 also shows the C_L curve of the Parafoil plus flares plus nylon cloth corrected to a RN of 3,000,000, corresponding to a velocity of 70 ft/sec. on a Parafoil having a chord length of 6'10".

Comparing the effects of the flares alone on the rigid airfoil and the rigid Parafoil shows that on both models they increased the slope of the lift curve, decreased $C_{L_{max}}$, and increased the drag slightly.

*Figures 36 and 37 show C_L data appearing like a stall. This reduction in lift is not a true stall phenomenon but is rather characteristic of testing a small model (c=5") in a low speed wind tunnel. In this case a laminar separation occurs which may be extrapolated to higher R_N by using the standard methods[4].

**Due to mounting, the data from the rigid Parafoil had to be shifted 2^o to the left.

The effect of the nylon cloth alone on the rigid airfoil and the rigid Parafoil was to increase the slope of the lift curve, and increase the drag.

The effect of the flares and the nylon cloth together was to increase the slope of the lift curve, and, increase the drag.

A comparison of the Parafoil Airfoil section and the conventional airfoil section showed that the Parafoil airfoil section decreased the slope of the lift curve, and increased the drag.

The rigid airfoil model variations produced an L/D range of 4.43 to 5.15. The rigid Parafoil model variations produced an L/D range of 3.90 to 5.0 .

There is a small reduction in the aerodynamic performance (L/D ratio) of the rigid Parafoil as compared to the rigid airfoil as evidenced by the increase in drag on the rigid Parafoil, and the decreased slope of the lift curve.

Data obtained from free flight tests carried out at the University confirmed Parafoil performance estimates based on the early wind tunnel data and also demonstrated lift to drag ratios in excess of four.[2,17,18]

The success of these early tests suggested that more extensive wind tunnel tests should be carried out on selected Parafoil designs.

Early NASA Tests

On the recommendation of Nicolaides, NASA obtained an original Parafoil kite[3] (Model 5) from Space Recovery Research Center, Inc., and undertook wind tunnel tests in the Langley 30 x 60 full scale wind tunnel in 1965. Some difficulty was experienced in rigging these models. The University was pleased to assist NASA in the rigging, and also loaned two of its Parafoil designs[3] (Models 6 and 7) for testing. The result of the NASA tests[3] are given in Ref. 3 and are also summarized in Figures 38 through 41. (Line drag removed)

Good agreement was obtained between the early Notre Dame wind tunnel tests[1] and the early NASA tests[3] on lift coefficient, drag coefficient and lift to drag ratio when line drag was removed from the Langley data, Fig. 69 and 82. In addition the Langley tests revealed that the Parafoil was statically stable over the entire range of test angles of attack from 0^{0} to 70^{0}.

Notre Dame Wind Tunnel Tests

Notre Dame/Air Force Wind Tunnel Tests

Static. The early wind tunnel tests and flight tests of the Parafoil led to a systematic wind tunnel test program of various Parafoil designs, ranging in aspect ratio from .5 to 3. This program was carried out for the U. S. Air Force Flight Dynamics Laboratory at the University of Notre Dame.

Wind tunnel models 3 and 4 were constructed of aluminum ribs and flares and the top and bottom surface of the model was composed of nylon cloth.* No rigging lines were used. The wind tunnel data from these tests is provided in Ref. 7.

Figure 42 provides a summary of the lift and drag coefficient data obtained on the variable aspect ratio Parafoil model 3. The data demonstrates the normal improvement in lift curve slope resulting from increasing aspect ratio. A summary of lift to drag ratios obtained from the various models is given in Figure 43. Again the improvement of lift to drag ratio with increasing aspect ratio is observed. Repeat tests are given in Figures 44 and 45 on Wind Tunnel Model 4. Summary curves on flap deflection are given in Figure 46.

Dynamic. Dynamic wind tunnel tests were carried out as described in an earlier section. The data from these tests are given in Ref. 8.

*Model 3 tested in 1967; model 4 tested in 1968.

A summary of results for the static pitching moment stability coefficient, C_{m_α}, is given in Figure 47 as a function of different trim angles of attack and for 3 locations of the confluence point below the Parafoil. A summary of the pitch damping moment stability coefficient ($C_{m_q} + C_{m_{\dot{\alpha}}}$) is given in Figure 48 for various trim angles of attack and for 3 locations of the confluence point.

The static and dynamic stability of the Parafoil is demonstrated by these unique wind tunnel tests.

NASA Langley Tests

During the period from 1964 through 1967 extensive flight tests of the Parafoil were carried out in order to obtain performance data to supplement the aerodynamic data from the wind tunnel testing program.[1,17] The results from both the wind tunnel tests and the full scale free flight tests led to a program of full scale Parafoil wind tunnel tests in the 30' x 60' NASA (Langley) full scale wind tunnel. This program was carried out by Notre Dame under the direction of the Air Force Flight Dynamics Laboratory commencing in the spring of 1968. The all fabric wind tunnel models 8 through 13 were designed by Nicolaides and were constructed under University supervision by the Dutron Corporation.

All of this data was transferred to IBM cards which were used in various computer programs. The various computer programs permitted the preparation of numerous plots. In this way data of different test conditions could be compared. Also, the various aerodynamic coefficients could be computed both with and without rigging line drag for comparison with previous wind tunnel tests. In addition special summary curves were prepared. For example, a summary plot of the wind tunnel data obtained on the aspect ratio 1 Parafoil at wind tunnel speeds of 30, 40 and 50 per second is given in Figure 49. Similar summary curves for the other aspect ratio models are given in Figures 50-53. Summary curves showing the effect of aspect ratio on lift coefficient and on lift to drag ratio are given in Figure 54 at a wind tunnel speed of 40 ft per second. An examination of this data suggests that some effects of speed or wing loading are indicated. Summary data for the various flap deflection effects is given in Figure 55 where it is noted that increases in the lift coefficient are obtained with increasing flap deflection as expected for basic wing theory. Figures 49-55 are prepared with line drag removed.

In order to improve Parafoil performance the leading edge opening* was

*Wind tunnel and flight tests at Notre Dame revealed better flight performance due to improved nose flow as observed in smoke photographs.

decreased by using 1" tape. The data resulting from this change in configuration is given in figures 56 through 59 for the aspect ratio 1 and the aspect ratio 3 models.

The strut tests enable determination of a restoring moment. A summary of the moment data is given in figure 62 and 109. The static pitching moment about the confluence point is plotted in figure 63 for confluence points located 1.5 span lengths below the Parafoil. Appendix I presents the method of performing this transformation of moments. See summary curves 60-61.

A summary of lift curve slope vs aspect ratio is provided in figure 64. The static yaw moment coefficient for aspect ratio 1,2,3 models is given in figure 65 which shows good stability. The static roll moment coefficient for side slip is given in figure 66 for 3 aspect ratio Parafoils. Again stabilizing moments are observed.

Qualitative

In addition to the aerodynamic force and moment coefficient data presented in the preceding paragraphs, numerous valuable visual observations were made. Of particular interest was the rigidity and self-inflation of the Parafoil over a large range of angles of attack. In the tether tests the Parafoil remained fully rigid and inflated over the entire range of test angles of attack, from -5^{o} to 70^{o}.

Any particular Parafoil is designed and rigged for a specific flight trim angle of attack. This design trim angle is generally near $+5^{o}$. When forced out of that trim angle by deflecting tether (Tether Tests) or by rotating strut (Strut Tests), the pennants and their lines will become slack and will flap, thereby causing unnecessary drag. The observations revealed that as the angle of attack is decreased below the design trim, the D lines first flap and then the C, and B.

At the large angles of attack the D lines first and then the C lines again flap. In a special test the D lines were disconnected and their pennants taped up. It was found that the Parafoil flew quite well with no flight stability or rigidity problems.

In the series of tests where the aspect ratio three Parafoil was cut off at the tips to yield lower aspect ratio units, the outside rib sections had their rib air passage vents exposed to the airflow, thus reducing the fabric internal pressure constraint. It was found that no change in inflation or stability resulted, and that the reduced AR sizes were as stable as the models with the complete non-porous outboard rib sections.

An investigation of the flow characteristics around the Parafoil was

made by taping wool tufts six inches in length on the upper surface of the Parafoil models at varied locations on the upper surface (Figure 31a). At low angles of attack the flow was clearly attached to the upper surface from leading edge of trailing edge. The flow remained attached until about $\alpha = 7.5^{o}$ (Fig. 31b). Between $\alpha = 7.5^{o}$ and $\alpha = 15^{o}$ the flow field changed significantly and is definitely unattached on the latter half of the upper surface.

Comparison of Tether and Strut Data Considerable differences are evident in comparing the L/D data obtained from the tethered tests (Fig. 54) with the data obtained from the strut tests (Fig. 61). In order to understand these and other differences in the Langley tests it is helpful to review some of the visual observations which were made during the runs.

Tether . During the tether tests the Parafoil models did not fly absolutely steady due to the gustiness of the tunnel flow, and the mount location in the rear of the tunnel. The tether mount system was located downstream in the test section where greater flow disturbances were prevalent. It was necessary, therefore to hand control the Parafoils with control lines attached to the rear. This controllability effect gave rise to residual motions resulting from the necessity to control the model so as to obtain a steady condition for the recording of a data point. Because of the multiplicity of data points recorded at a given angle of attack, all points at the same angle of attack were averaged to yield one representative data point per α. The angle of attack of the Parafoil was assumed to be the same as the right wing tip which was measured from side view photographs. The angle was noted to vary by as much as $\pm\ 3^{o}$ at a given test condition. In addition, the models were not trimmed to optimum performance conditions at each angle of attack. Hence, it is believed that all of these factors account for the scatter and inconsistencies apparent in the tether results.

The tether technique was employed to check general Parafoil rigidity and performance (e.g. flight stability, trim, trim change, yaw and roll control, etc...). It should not, however, be used in a quantitative manner but rather as confirmation of general Parafoil aerodynamics.

The tether tests, through visual observations and movies, clearly confirmed controllability in yaw, roll, and pitch. The static and dynamic stability of the Parafoils was observed for numerous pitch trim positions and for numerous yaw and roll trim positions.

Strut. In the strut tests the angle of attack of the Parafoil was measured by two means: (1) by photographing the right wing tip (α_V), and (2) by photographing the main bar support (which was positioned so as to always be perpendicular to the mid-span chord line), (α_S). For angles of attack between 11^O and 20^O, α_S and α_V are in good agreement. Figures 67-68 illustrate the shifting of the lift curve and the lift to drag curve as a result of the angle of attack measurement technique. However, for angles of attack less than 11^O, $\alpha_V > \alpha_S$, and for angles of attack greater than 20^O, $\alpha_V < \alpha_S$. The method of strut support utilized rigid tie bars which were attached to the Parafoil at its mid-area. Because of this rigid attachment the Parafoil was not completely free to move to the proper trim angle when the strut angle of attack was changed. As a result the Parafoil was physically distorted and thus its angle of attack distribution was distorted. It was observed that when the model was pitched at a negative angle of attack, the angle of attack of the outboard wing tips was greater than the angle of attack of the mid-span. When the model was pitched to a high angle of attack, the angle of attack of the outboard wing tips was less than that of the mid span. Although this phenomenon might be attributed to the flow field around a non-rigid body such as the Parafoil, it was observed from test film that this was a characteristic resulting from the strut mount arrangement. As previously discussed a given Parafoil is designed for a particular trim angle of attack. That is to say the pennant design and the rigging lines are related to a certain confluence point which is determined by the design trim angle of attack. Once the Parafoil is constructed there is nothing which can be done to change this optimum design. The use of a rigging platform, as employed in the strut tests, simply simulates the design confluence point and thus permits the Parafoil to fit in the available wind tunnel test section area. Any movement of the Parafoil to an angle of attack other than the design trim angle results in an off design condition and results in a forced distortion of the Parafoil from its desired flight position. This distortion was readily observed during the tests and could be seen in the test film. Therefore the strut data is highly suspect at the low angles of attack ($\alpha < 5^O$) tested. All strut data unless otherwise specified was plotted versus α_V and each data point represents a recorded data point, that is, no averaging technique was incorporated for values at the same angle of attack.

WIND TUNNEL TEST SUMMARY

Summary curves of wind tunnel data as obtained from the various tests conducted at both the University of Notre Dame, and at NASA have been presented. However, the data from these various programs are not in complete agreement. As a result, general summary curves representing aerodynamic performance of the Parafoil are now given.

Lift Summary

Figures 69 and 70 give a complete summary of all the lift coefficient data. Figures 71 through 81 present the supporting data for the summary curves, and the representative lines used.

Lift to Drag Ratio Summary*

A general summary of the lift to drag ratio data without line drag is given in Figure 82. The supporting data for determining the representative curve data is given in Figures 83 through 93. Figures 107 and 108 present a general summary of this data with line drag effects included.

Drag Summary*

The general summary of wing alone drag data is given in Figure 94, and the supporting curves are given in Figures 95 through 105. Figure 106 presents a general summary of this data including line drag effects.

Moment Summary

The static moment of the wing alone over the full range of angles of attack is shown in Figure 109. Supporting curves are given in Figures 110-114. The same data transferred to a confluence point 1.5 spans** below the Parafoil is illustrated in Figure 63. Supporting curves are given in Figures 115-119.

---

*Parafoil models used in the tests conducted at Notre Dame contained proturbences which produce a drag component not taken into consideration in these lift to drag or drag data presentations. Appendix IV includes an analysis of the effects of correcting the data to reflect removal of this additional drag.

**Flight Parafoils now utilize a 1.0 span confluence point. Also the lines are of reduced number and diameter. Accordingly, all Parafoils of any aspect ratio are able to achieve static stability over their entire range of angles of attack.

PARAFOIL FLIGHT SYSTEMS

Incorporation of the Parafoil into a flight system requires consideration of line and payload drag created by the configuration of the intended system. Appendix V illustrates incorporation of line drag data for a personnel size Parafoil.

CONCLUDING REMARKS

A summary of Parafoil wind tunnel data has been presented. Data from the various wind tunnel testing programs has been reduced to a common basis and numerous comparison plots have been prepared which illustrate the effects of aspect ratio, velocity, trim angle, control deflection and configuration.

The aerodynamic data confirms that the Parafoil is similar to the airplane wing. The Parafoil has positive lift at zero angle of attack. Figures show lift down to about -5^{o}. The lift curve is quite linear with angle of attack. Increasing the aspect ratio increases the lift curve slope and improves the lift to drag ratio. The Parafoil has static and dynamic stability in all modes of flight, pitch, yaw, and roll.

The Parafoil, because of its configuration and flexibility, does not exhibit the stall characteristics of the aeroplane wing at large angles of attack. Instead the lift falls off gently and thus the Parafoil may also be safely flown at very large angles of attack ($70^{o}+$).

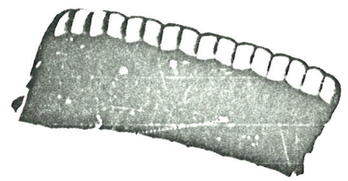

Figure 1a. Parafoil in Gliding Flight.

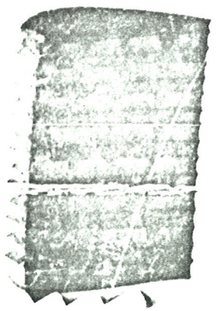

Figure 1b. Parafoil in Gliding Flight.

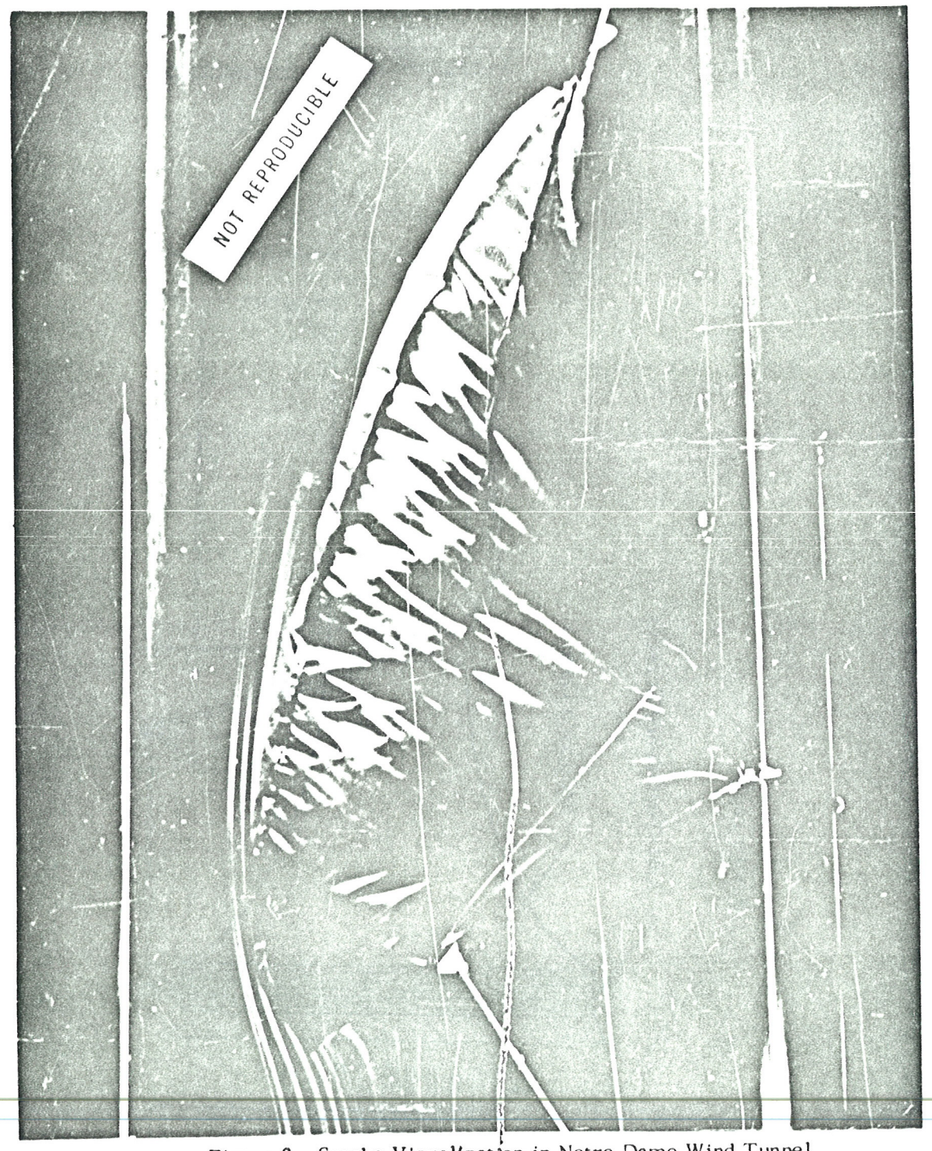

Figure 2. Smoke Visualization in Notre Dame Wind Tunnel

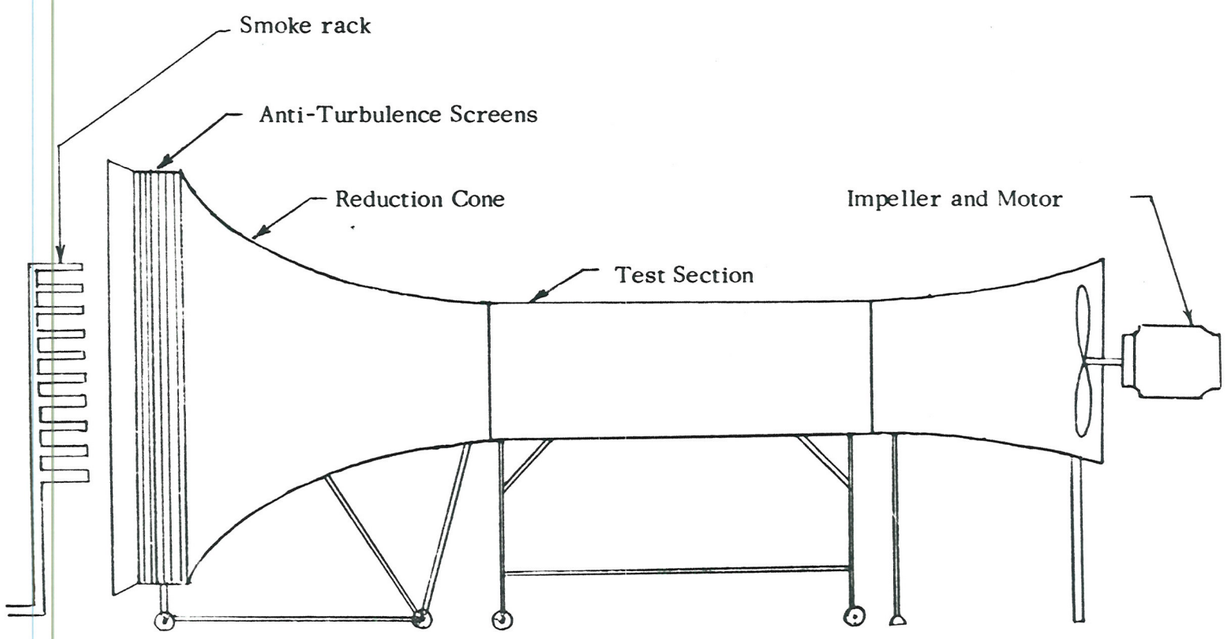

Figure 3. Schematic of Notre Dame Wind Tunnel

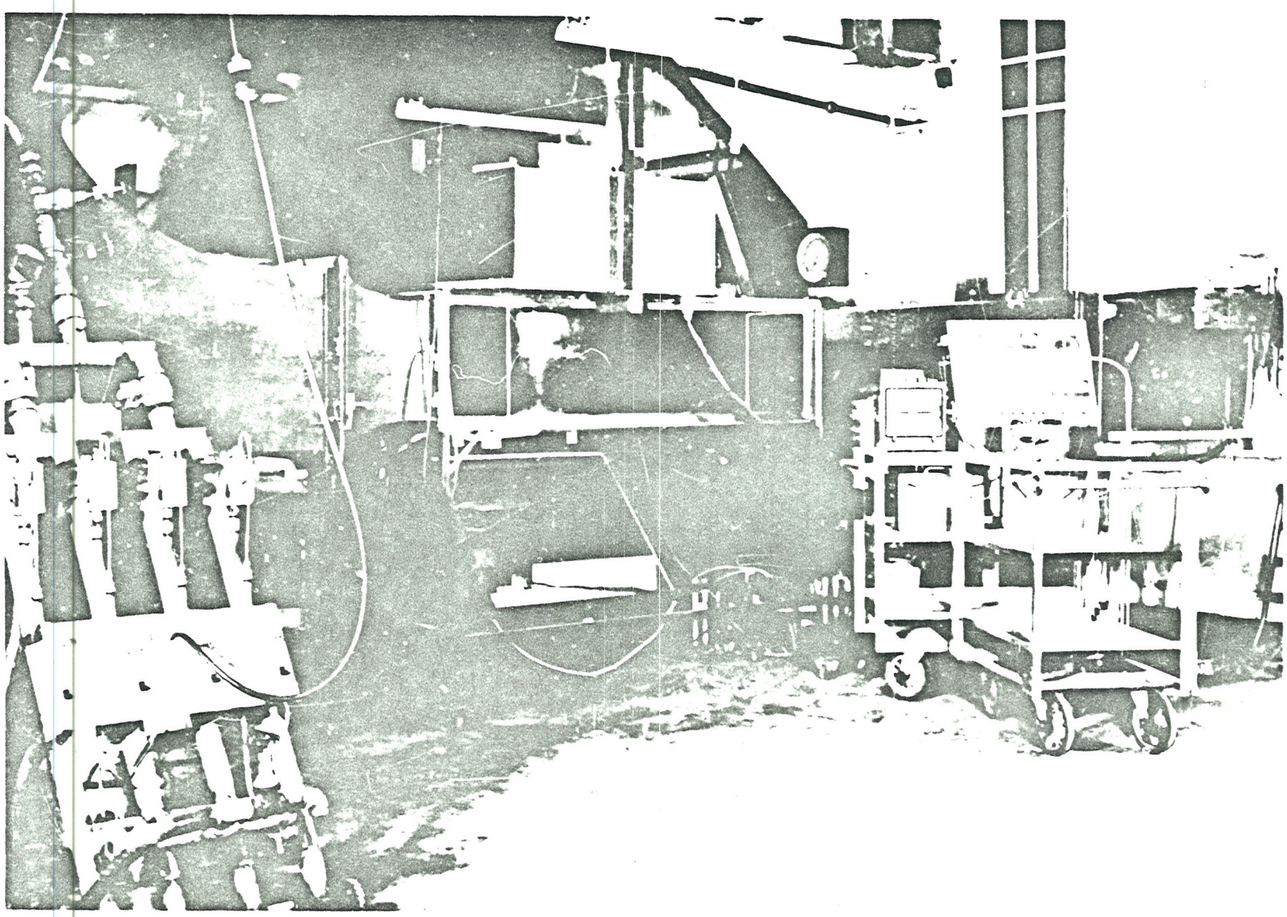

Figure 4. Notre Dame Wind Tunnel

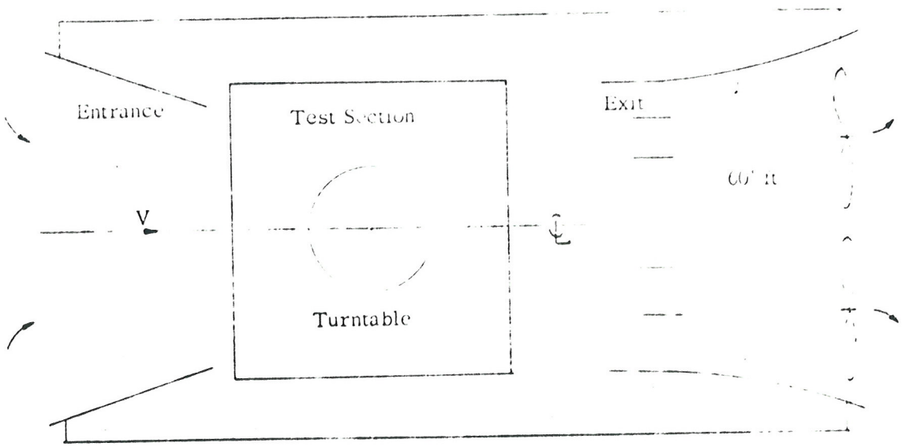

(a) Top Profile

(b) Side Profile

Figure 5. Langley Full-Scale Tunnel

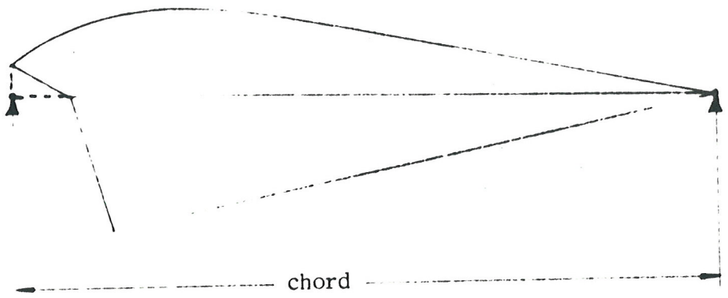

AIRFOIL	
Station	Ordinate
0.0000	0.0481
.0481	.0769
.0769	.0962
.0962	.1106
.1442	.1202
.1731	.1250
.1923	.1269
.2404	.1202
.2885	.1144
.3365	.1077
.3846	.1010
.4327	.0981
.4808	.0962
.5288	.0913
.5769	.0865
.6250	.0750
.0731	.0673
1.0000	.0000

Figure 6. Parafoil Model 1 Airfoil Section and Dimensions (in fraction of chord).

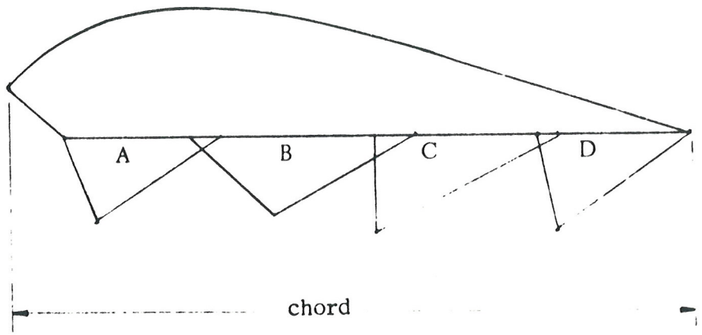

AIRFOIL	
Station	Ordinate
.0000	.0677
.0322	.1048
.0645	.1322
.0806	.1455
.1290	.1661
.1612	.1774
.2258	.1887
.2580	.1919
.2903	.1887
.3225	.1854
.4032	.1774
.4838	.1629
.5645	.1435
.6451	.1209
.7258	.0983
.8064	.0725
.8870	.0435
1.0000	.0000

Figure 7. Parafoil Model 2 Airfoil Section and Dimensions (in fraction of chord)

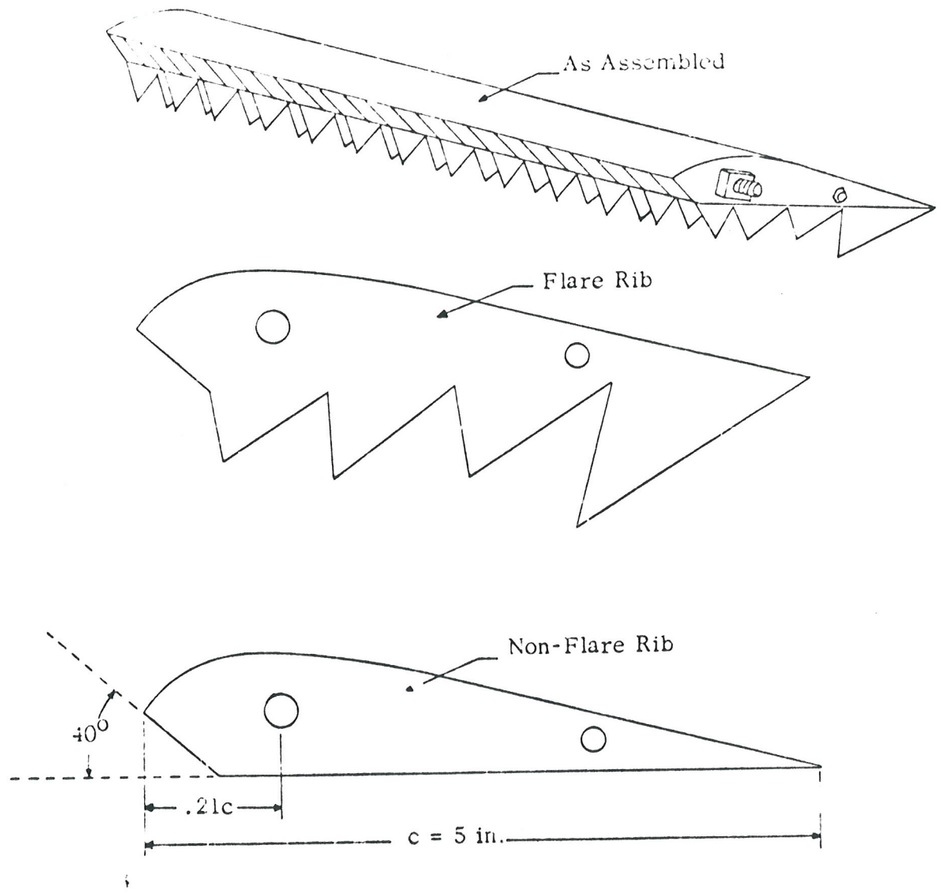

Figure 8. Para-Foil Model Assembly (Models 3 and 4)

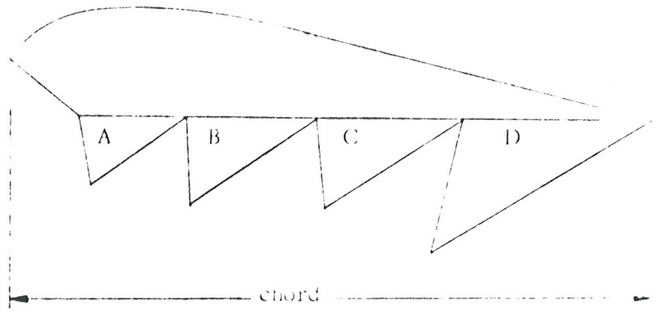

AIRFOIL	
Station	Ordinates
0.	0.0856
.0200	.1200
.0400	.1592
.0600	.1518
.0800	.1616
.1000	.1658
.1056	.0000
.1200	.1730
.1400	.1756
.1600	.1780
.1800	.1784
.2000	.1790
.2200	.1790
.2400	.1768
.2600	.1752
.2800	.1730
.3000	.1705
.3200	.1676
.3400	.1646
.3600	.1605
.3800	.1562
.4000	.1523
.4200	.1476
.4400	.1426
1.0000	0.0000

Figure 9. Parafoil Models 3 and 4 Airfoil Section and Dimensions
(In fraction of chord)

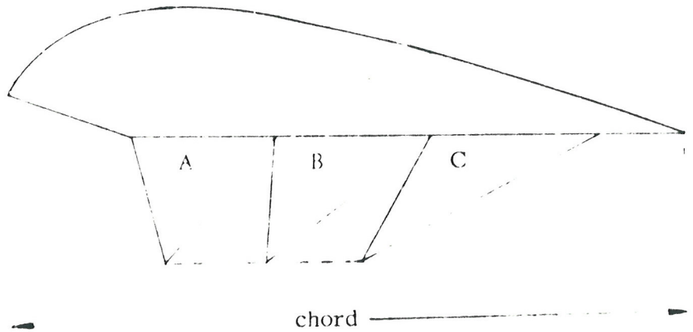

AIRFOIL	
Station	Ordinate
0.0000	0.0606
.0125	.0888
.0250	.1095
.0500	.1331
.0750	.1539
.1000	.1642
.1500	.1805
.2000	.1953
.2500	.2012
.3000	.1953
.4000	.1805
.5000	.1539
.6000	.1317
.7000	.1065
.8000	.0740
.9000	.0385
1.0000	.0000

Figure 10. Parafoil Model 5 airfoil Section and Dimensions (in fraction of chord)

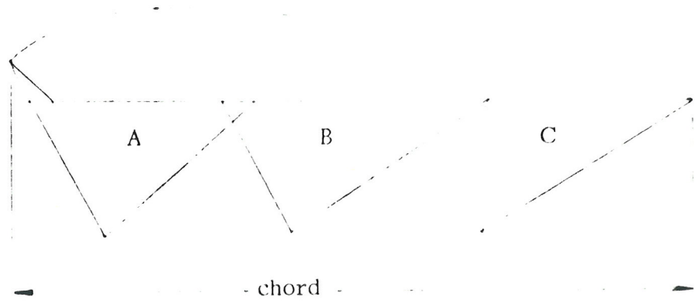

AIRFOIL	
Station	Ordinate
0.0000	0.0594
.0125	.0648
.0250	.0777
.0500	.0899
.0750	.1007
.1000	.1079
.1500	.1169
.2000	.1223
.2500	.1259
.3000	.1259
.4000	.1223
.5000	.1133
.6000	.0950
.7000	.0763
.8000	.0504
.9000	.0288
1.0000	.0000

Figure 11. Parafoil Model 6 Airfoil Section and Dimensions (in fraction of chord)

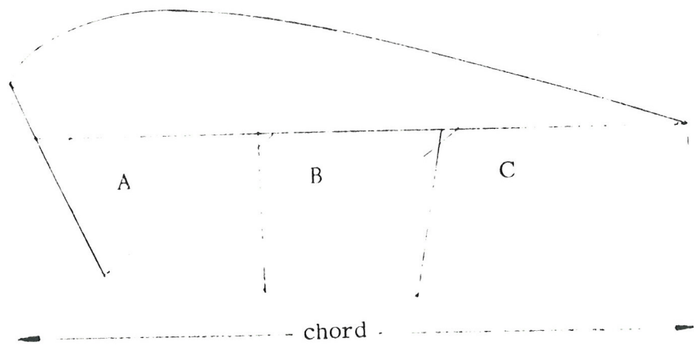

AIRFOIL	
Station	Ordinate
0.0000	0.0811
.0125	.1081
.0250	.1208
.0500	.1399
.0750	.1526
.1000	.1622
.1500	.1749
.2000	.1812
.2500	.1844
.3000	.1812
.4000	.1653
.5000	.1437
.6000	.1208
.7000	.0916
.8000	.0604
.9000	.0286
1.0000	.0000

Figure 12. Parafoil Model 7 Airfoil Section and Dimensions
(in fraction of chord)

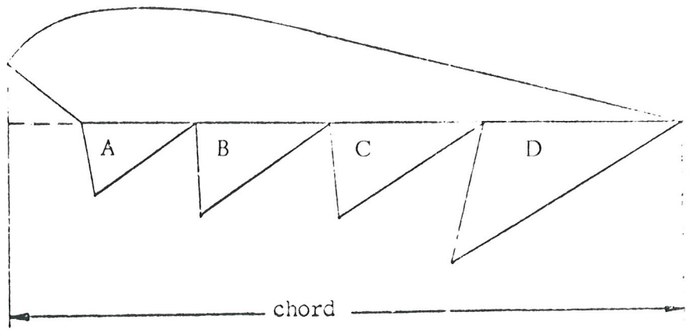

AIRFOIL	
Station	Ordinates
0.	0.0886
.0200	.1206
.0400	.1392
.0600	.1518
.0800	.1616
.1000	.1688
.1056	.0000
.1200	.1730
.1400	.1756
.1600	.1780
.1800	.1784
.2000	.1790
.2200	.1790
.2400	.1768
.2600	.1752
.2800	.1730
.3000	.1703
.3200	.1676
.3400	.1646
.3600	.1606
.3800	.1562
.4000	.1524
.4200	.1476
.4400	.1426
1.0000	0.0000

Figure 13. Parafoil Models 8-13 Airfoil Section and Dimensions (in fraction of chord)

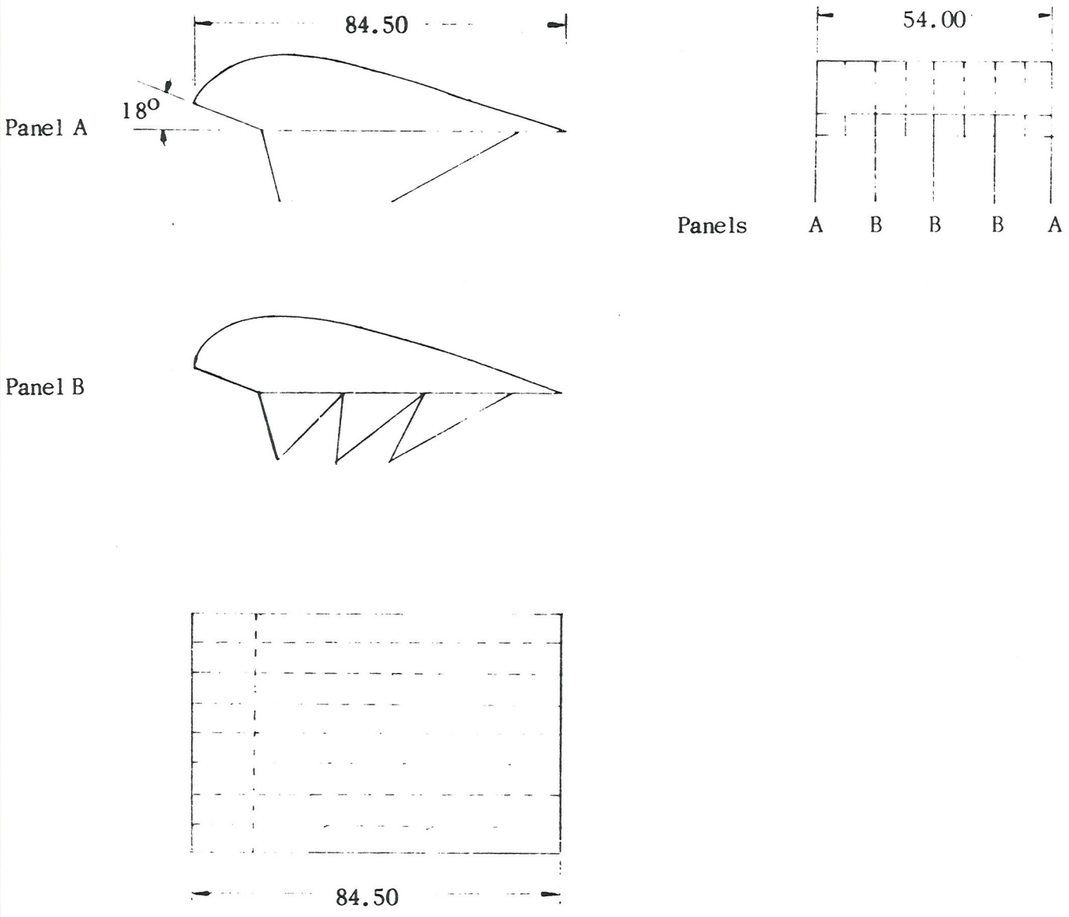

Figure 14. Para-Foil Model 5. Dimensions in inches

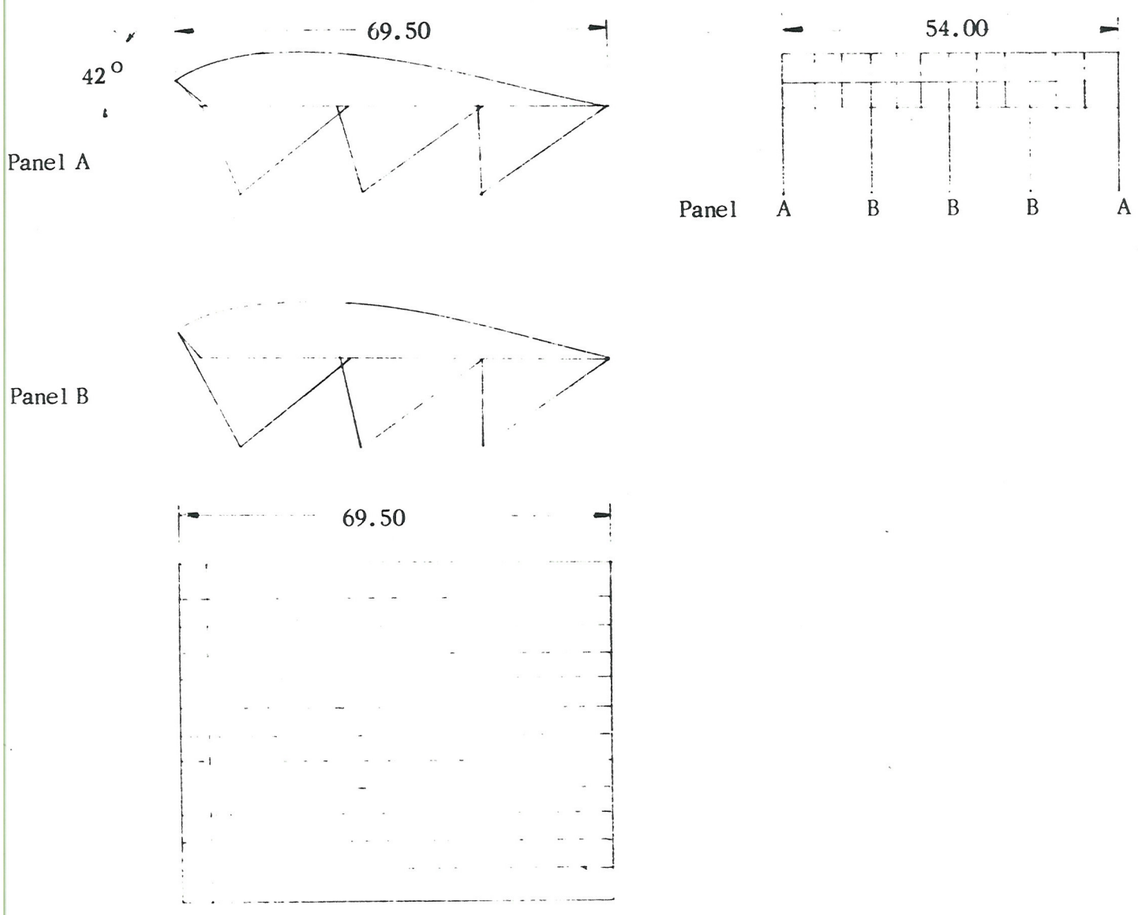

Figure 15. Para-Foil Model 6. Dimensions (in inches)

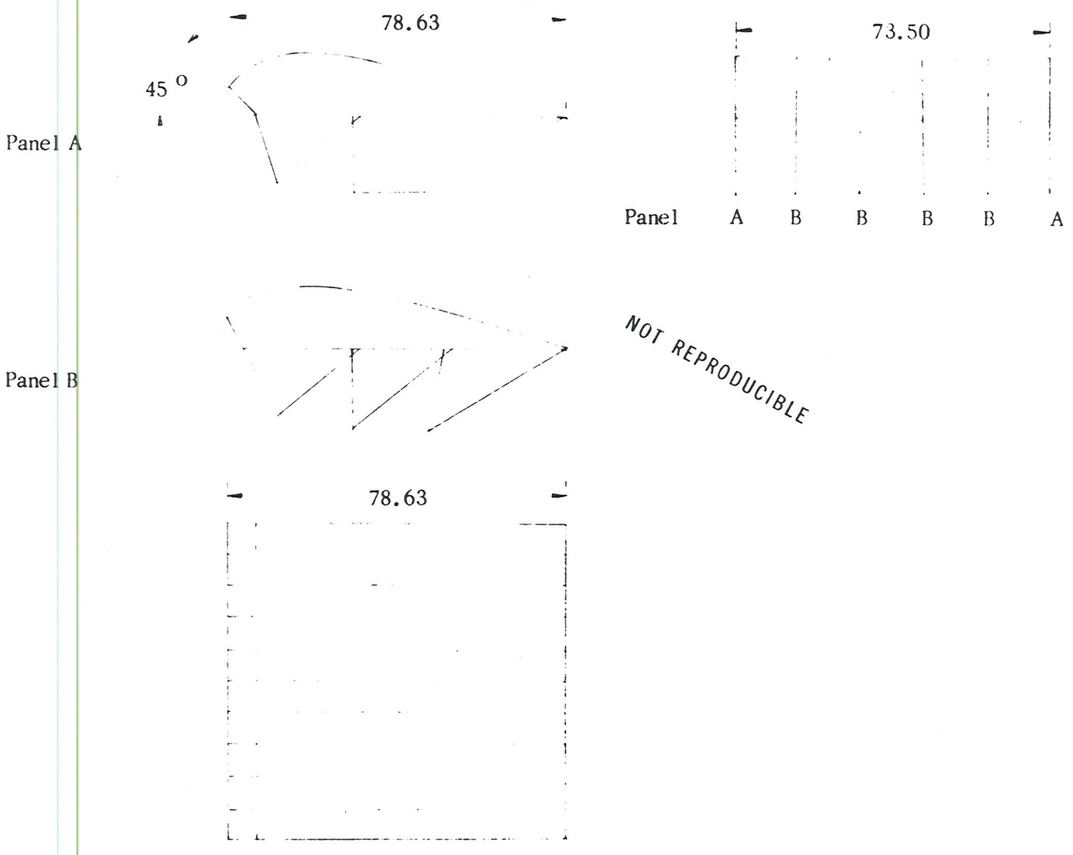

Figure 16. Para-Foil Model 7. Dimensions (in inches)

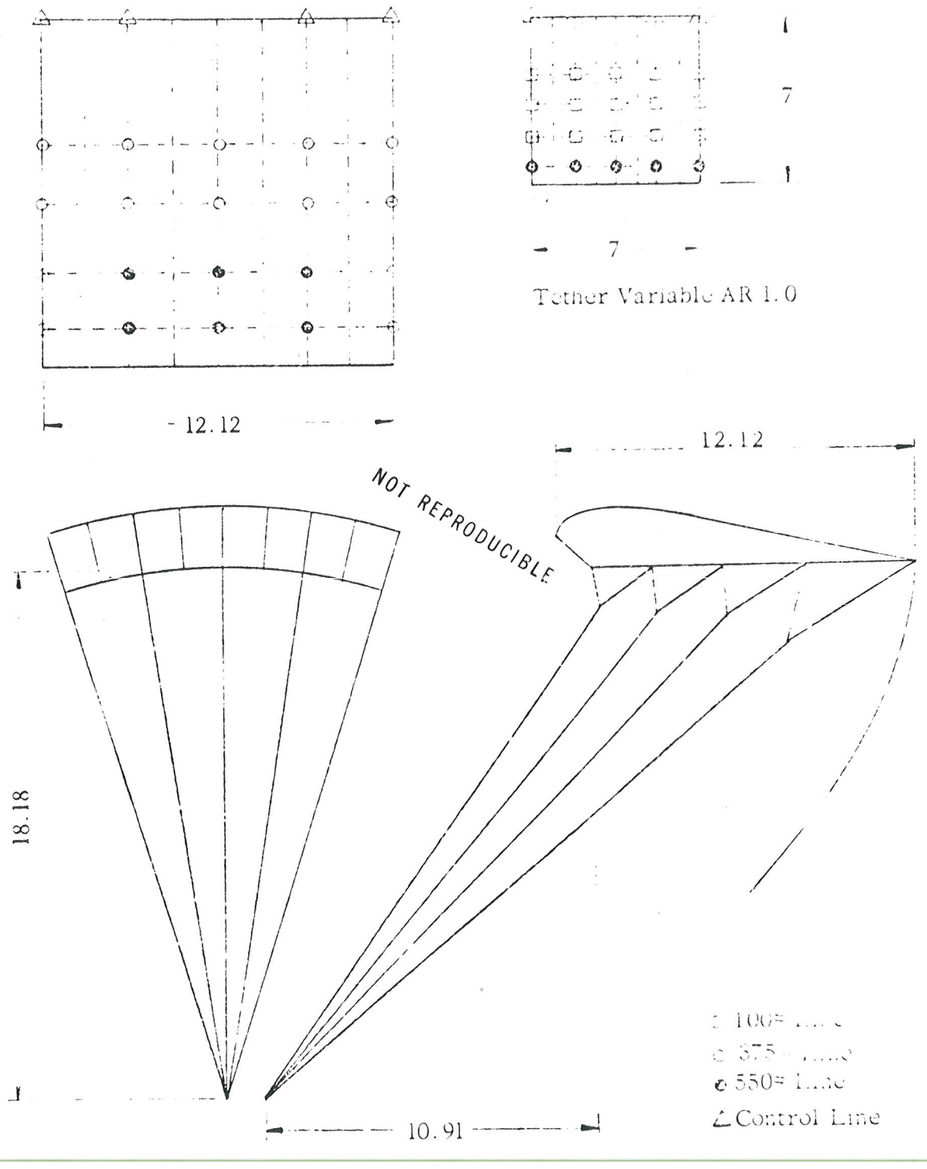

Figure 17. Model 8 : AR 1.0 (Dimensions in feet)

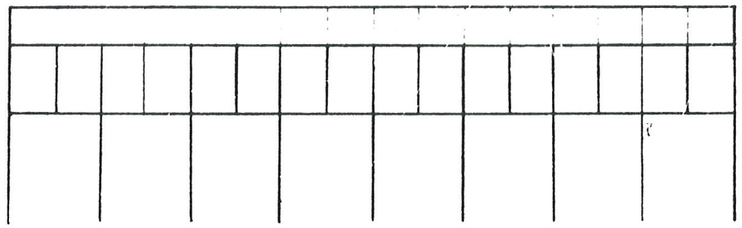

1.) Not Taped

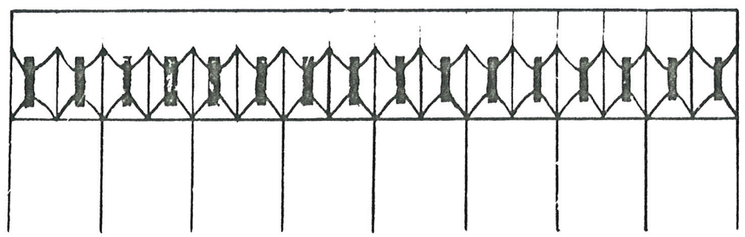

2.) Leading edge taped 33% closed

Figure 17a. Tape on Leading Edge.

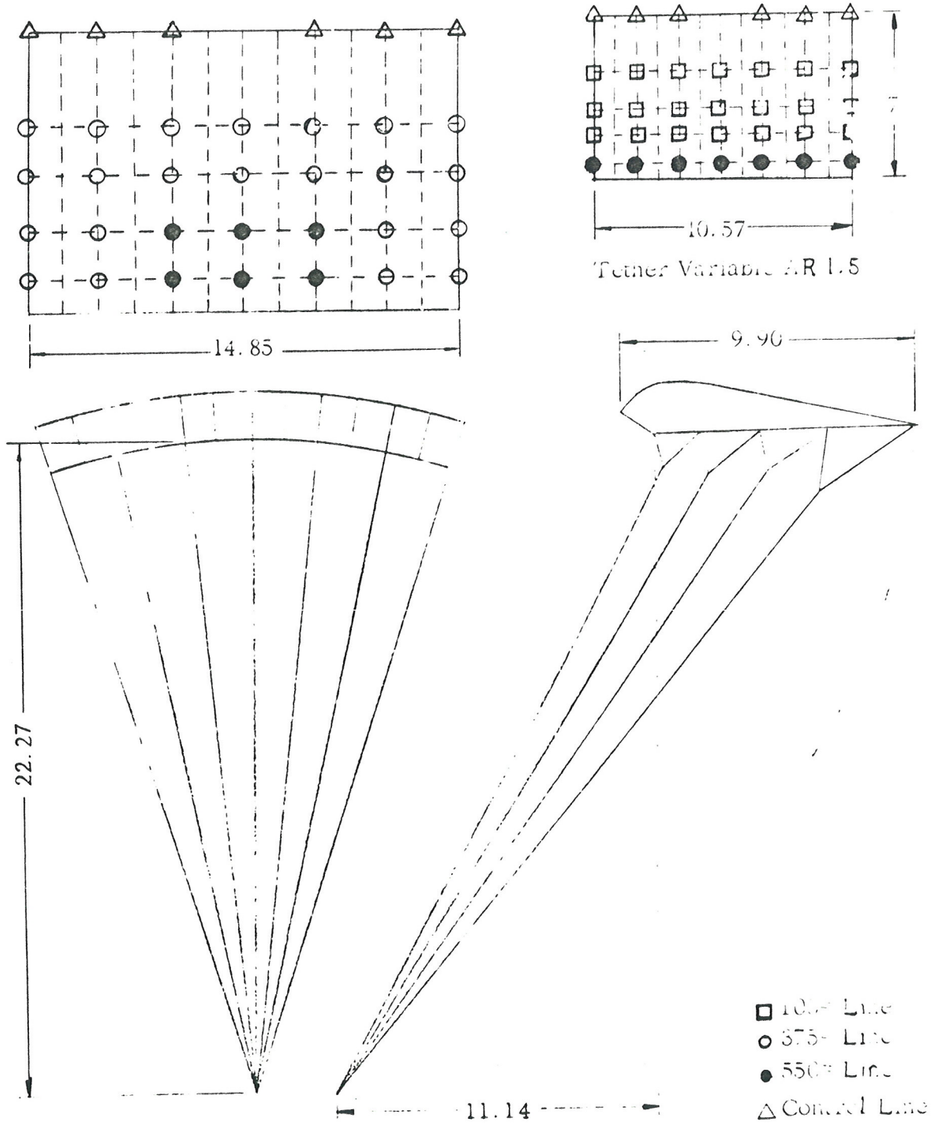

Figure 18. Model 9 : AR 1.5 (Dimensions in feet)